UDC 621.923.74 **doi: 10.20998/2078-7405.2024.100.09**

ANALYSIS OF THE ABBOTT-FIRESTONE CURVE ON A DIAMOND-BURNISHED SURFACE

Szilárd **Smolnicki**, Gyula **Varga** [0000-0003-3810-2881]

University of Miskolc, 3515 Miskolc-Egyetemváros, Hungary
gyulavarga@uni-miskolc.hu

Received: 25 March 2024 / Revised: 21 April 2024 / Accepted: 26 May 2024 / Published: 15 June 2024

Abstract. *In the research we provide a brief overview of the context of the topic, starting from the issues of energy efficiency and environmental awareness and sustainable development, through the positive properties of alternative forms of processing such as diamond burnishing, to the examination of the surface finish, which plays a key role in the relationship between surface quality and diamond burnishing. In the first chapter of this paper, the science of sustainable development, industrial ecology and its different systems models are presented, leading to the three pillars of sustainable development. In the same chapter, we touch on the relationship between energy- and eco-efficiency, their characteristics, recent research results and impacts. We present the dimensions and material quality of the test piece on which the tests were carried out. This will be followed by a description of the technological characteristics of the turning and diamond-burnishing processes. The characteristics and usefulness of the Abbott-Firestone curve are listed, and the improvement factors and K-coefficients are calculated. In the third section, experimental results are presented by examining the data of the Abbott-Firestone surface curves, which are presented using both the improvement factors and the K-coefficients to draw conclusions by examining the different technological parameters. We conclude our study by summarizing the results of our research.*

Keywords: *energy efficiency; sustainable development; slide diamond burnishing; surface finish.*

1. Energy efficiency issues

1.1. About sustainable development

Industrial ecology, also known as the science of sustainability, is primarily concerned with the harmonisation of natural and industrial systems, based on a wide range of objective information on the performance of and interrelations between the two systems [1]. Its history goes back to the middle of the 20th century, when a report published in 1972 predicted unsustainable demand and production, a worldwide increase in pollution, depletion of natural resources, widespread malnutrition, and a growing world population [2]. In 1987, the report of the commission chaired by Gro Harlem Brundtland defined sustainable development as development that meets the needs of the present without compromising the ability

of future generations to meet their own needs [3]. Then in 1989, Schaltegger and Sturm examined sustainable development in an eco-efficiency approach, the idea being that goods and services are of greater value if they produce less waste and pollution [4]. The 1992 United Nations Conference on Environment and Development in Rio de Janeiro produced the "Agenda 21" report, one paragraph of which stated that 'achieving the goals of environmental quality and sustainable development will require efficiency in production and changes in consumption patterns, with a focus on optimising resource use and minimising waste' [5].

Industrial ecology is thus how humanity can approach and maintain consumer needs in the face of continuous economic, cultural, and technological development; while the concept requires that an industrial system be considered in harmony with, rather than in isolation from, its surrounding systems [1]. Its essence can be illustrated by presenting three different system models, as shown in Figure 1. Type I is a linear system, where resources are implanted in unlimited quantities, which are disposed of as waste after use. In a Type II system, on the other hand, internal cycles are created and there will be significant internal reuse of materials, so that the amount of material entering and leaving the system can be limited. In a Type III system, full material cycling is achieved, where only energy input is required [1].

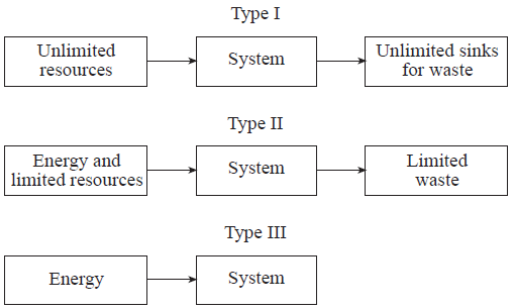

Figure 1. Industrial ecology system types [6]

Sustainable development is not a recent concept, but its achievement still seems very far away even today. The reasons for this are to be found in its three pillars, as shown in Figure 2. Aligning society, the environment and the economy is not easy, and changes in any one of them can upset the balance, because development wants to be liveable, equitable and eco-efficient at the same time.

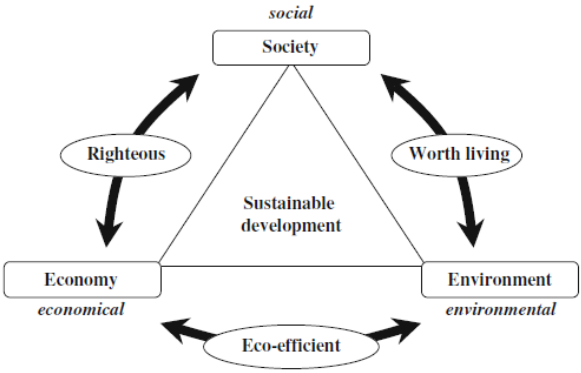

Figure 2. The three pillars of sustainable development [7]

1.2. From energy efficiency to eco-efficiency

The eco-efficiency of a process resolves an apparent contradiction through appropriate innovations and approaches: it "seeks development that allows for an increase in well-being for all while reducing the use of nature" [1].

The reasons for pursuing eco-efficiency are summarised in the following list [8, 9]:

- to attract the attention of companies by encouraging them to innovate,
- to encourage innovation to stimulate innovation, to overcome market failures, external costs, public goods provision, information, and adaptation gaps,
- generate knowledge about likely resource efficiency gaps and potential areas for improvement,
- create and stabilise demand for environmental improvements,
- levelling the playing field in transition periods between technological development paths,
- increasing the likelihood of a new direction of technological development,
- maintaining the policy function of more stringent measures in cases where the state of the environment continues to deteriorate, or new negative external costs emerge.

Eco-efficient perceptions are also leading companies to rethink quality. By recycling and reusing materials that were previously accepted as by-products in processes, they unleash the power of innovation and quality management, for example in waste management, so that the redistributed knowledge base can be used in the actual production itself, as a by-product of change, such as the replacement or reuse of production inputs, increased process yields, careful monitoring and maintenance, and product improvement [10].

To summarise, seven essential guidelines for eco-efficiency can be distinguished [11]:

- reducing the material intensity of goods and services,
- reducing the intensity of goods and services,
- reducing the dispersion of toxic substances,
- reduce the recyclability of materials,
- maximise the sustainable use of renewable resources,
- extend the durability of products,
- increase the service intensity of products.

In addition to these guidelines, indirect elements such as a new perspective on human needs and quality of life, recognition of the capacity limits of ecosystems, and the continuous development of the concept to reflect its dynamic nature are also important [10].

The environmental equivalent of the concept of zero defects in quality insurance is nothing less than zero emissions of hazardous or potentially hazardous substances from a facility or product. Although this is almost impossible, the eco-efficient approach seeks to minimise waste emissions [11]. Practice shows that these guidelines are often in sync with consumer needs, as the size of electronic devices tends to decrease with the development of computing, while the proliferation of digital storage devices (flash drives, hard disks) will eventually eliminate paper-based documentation.

The standard DIN EN ISO 14045 deals with the assessment of eco-efficiency, an approach that can be applied to the assessment of the relationship between certain economic values and the environmental impact of manufacturing processes and systems. The assessment consists of five phases [12, 13]:

(1) definition of purpose and scope,
(2) environmental assessment,
(3) product system value assessment,
(4) quantification of eco-efficiency and
(5) interpretation.

The purpose and scope statement (1) defines the purpose of the eco-efficiency evaluation, the target audience, and the intended use of the results. The environmental assessment (2) is used to determine the potential environmental impact of the product system. The product system value assessment (3) considers the whole life cycle of the product system by assessing the value or desirability of the functional, monetary or other values assigned. In quantifying eco-efficiency (4), the ratio between the results of the environmental assessment and the assessment of the value of the product system is determined in accordance with the definition of the objective and scope [12, 13]. However, the perspective from which the ratio of environmental impact to product quality is ultimately interpreted (5) may differ.

Some research refers to eco-efficiency as eco-productivity, since many economists consider the environment (including natural resources) as a factor of production, and thus formulate eco-productivity as the welfare output of goods and services per unit of environment consumed [14]. The inverse of this, eco-intensity, is closer to the engineering approach, and refers to the use of natural resources per unit of welfare output [1].

Nor are the basic concepts of thermodynamics true in this case, since market conditions are determined by people's capricious preferences (e.g. a torn pair of jeans is more valuable than a spotless pair), which therefore changes the demand function and prices. Furthermore, since companies link their performance evaluation to environmental performance, it is worthwhile to choose a measure of eco-productivity in terms of $\frac{CO_2}{kg}$ or $\frac{resource}{kg}$ [14].

2. Surface machining and roughness measurement

2.1. Characteristics of the test piece

After a theoretical overview, we now turn to the experiments, for which a special axial part designed for this purpose was machined, the technical drawing of which is shown in Figure 3. The part was designed with six cylindrical surfaces where measurements can be taken and was manufactured on machine tools at the workshop of the Institute of Manufacturing Science of the University of Miskolc. A total of four pieces were made.

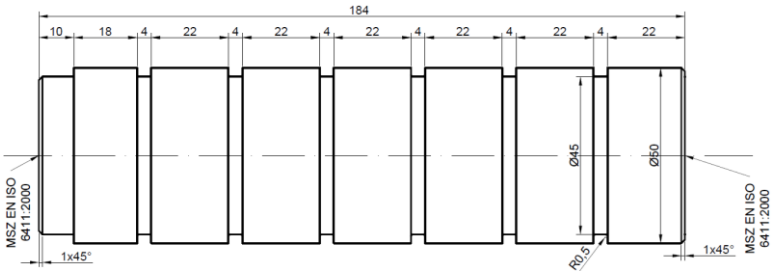

Figure 3. Technical drawing of the test specimen

The material used for the machining was austenitic stainless chromium-nickel steel alloy with a fabricated structure, designated 1.4307 (further designations: X2CrNi18- 9/304L/S30403), which has good corrosion resistance properties and is well suited to cold forming and welding. Due to its excellent anti-fouling properties, resistance to oxidation and easy cleanability, it is often used for food processing equipment (brewing, dairy, wine making), kitchen equipment and

appliances and chemical equipment (containers, heat exchangers, soap making). Its chemical composition is summarised in Table 1 [15].

Table 1. Chemical composition (at 20 °C) - DIN 10088-1:2005 [15]

Element	**Fe**	**C**	**Si**	**Mn**	**P**	**S**	**N**	**Cr**	**Ni**
%	66.8-71,3	≤0.03	1	2	0.045	0.015	≤0.11	17.5-19.5	8-10.5

The yield strength of an alloy $R_{p0,2} \geq 210\ MPa$; its tensile strength $R_m = 520 - 700\ MPa$, while its elongation at break is $A \geq 45\%$. Its density $\rho = 7.9\ kg/dm^3$, its hardness is $160 - 190\ HB$.

2.2. Features of turning

Machining started with sawing the parts to size, then continued with the centre hole on the left side of the part and the machining of the diameter for the clamping on the EU-400-01 lathe. This was followed by longitudinal turning in =Ø50 mm, and then the plunge-cutting starting from the right end of the part every 22 mm.

The technological parameters of the lathe were set up as follows for the surfaces to be measured:

- $v_c = 1.3875 \left[\frac{m}{s}\right]; f = 0.05\ \frac{mm}{revolution}$

In total, 24 surfaces (4 test pieces, 6-6 surfaces per test piece) were turned under the same conditions.

2.3. Features of diamond burnishing

Diamond burnishing used to replace low productivity and costly machining operations (grinding, mirror finishing, polishing) as a finishing operation for high precision and low roughness working surfaces. The advantage of diamond tools is that they have a very low coefficient of friction when friction is applied to metal surfaces, which allows the surface to be polished to low roughness [16].

After turning, the test pieces were not immediately machined by diamond burnishing, but roughness measurements were taken beforehand to compare them with the results of diamond burnishing to obtain a more accurate picture of the effectiveness of diamond burnishing. The methodology of the comparison and the roughness measurements are described in the following chapters.

The diamond burnishing was carried out using the same EU-400-01 type EU-400-01 lathe with a clamped burnishing tool. The head of the burnishing tool was a single-grain diamond, and the machining conditions are schematically illustrated in Figure 4 [17]. In the figure, 1 is the workpiece, 2 the burnishing tool, 3 the burnishing insert, 4 the tool clamp and 5 the diamond tip.

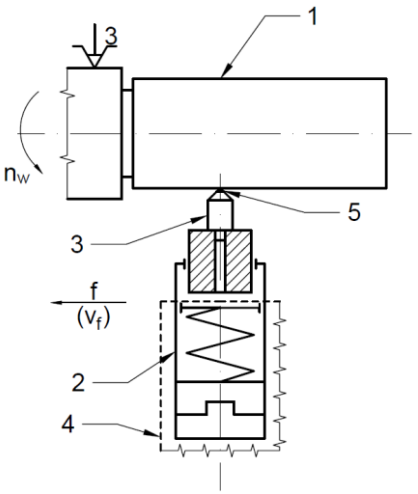

Figure 4. Schematic diagram of diamond burnishing [17]

During surface burnishing, the reduction of surface roughness and the hardening of the surface layer is caused by the sliding friction between the diamond tool and the workpiece surface, which is much harder than the material to be machined [18].

The technological data for diamond burnishing were different for each surface, which were the result of combinations of rate of rotation, feed rate and burnishing force exerted by the burnishing tool. These combinations are summarised in Table 2. The marking of the surfaces was grouped by hexadecimal using the test pieces. Two calculated values were also added to the table, the burnishing speed – formula (1) – and the machining power – formula (2).

$$v_v = d \cdot \pi \cdot n \left[\frac{m}{s}\right] \quad (1)$$

$$P = F \cdot v_v \quad (2)$$

Table 2. Technological data for diamond burnishing

Serial Nr.	$f\ \left[\frac{mm}{rev}\right]$	$n\ \left[\frac{1}{min}\right]$	$v_v\ \left[\frac{m}{s}\right]$	$F\ (N)$	$P\ (W)$
1-1	0.05	265	0.6938	120	83.25
1-2	0.05	265	0.6938	100	69.38
1-3	0.05	265	0.6938	80	55.50
1-4	0.05	265	0.6938	60	41.63
1-5	0.05	265	0.6938	40	27.75
1-6	0.05	265	0.6938	20	13.88

2-1	0.1	265	0.6938	120	83.25
2-2	0.1	265	0.6938	100	69.38
2-3	0.1	265	0.6938	80	55.50
2-4	0.1	265	0.6938	60	41.63
2-5	0.1	265	0.6938	40	27.75
2-6	0.1	265	0.6938	20	13.88
3-1	0.05	375	0.9817	120	117.81
3-2	0.05	375	0.9817	100	98.17
3-3	0.05	375	0.9817	80	78.54
3-4	0.05	375	0.9817	60	58.90
3-5	0.05	375	0.9817	40	39.27
3-6	0.05	375	0.9817	20	19.63
4-1	0.1	375	0.9817	120	117.81
4-2	0.1	375	0.9817	100	98.17
4-3	0.1	375	0.9817	80	78.54
4-4	0.1	375	0.9817	60	58.90
4-5	0.1	375	0.9817	40	39.27
4-6	0.1	375	0.9817	20	19.63

2.4. Measurement of surface roughness

The concept of surface quality encompasses the deformations, roughness and waviness of the machined surface [19]. In the following, the main 2D and 3D roughness metrics are presented, so that we can then compare the individual characteristics based on certain considerations. These are given in micrometres.
The characteristics of the Abbott-Firestone Curve (AFC) are described in ISO 13565, which divides the surface curve into peak, core and valley zones [20]. Accordingly, there are three surface roughness characteristics that provide information on the material content of the surface. These are:

- R_k: core roughness depth
- R_{pk}: reduced peak height
- R_{vk}: reduced valley height

As shown in Figure 5, each parameter is a projection of the material portion curve. The core roughness depth of the profile is obtained where the slope of the barrel surface curve is the smallest. This forms the peak zone to the left and the valley zone to the right, which have a significant slope

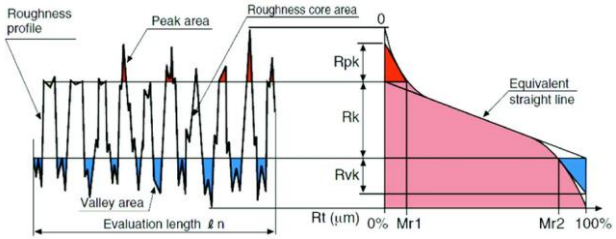

Figure 5. Abbott-Fireston Curve parameters for 2D case [20]

Due to the sensitivity to outliers, and parameters R_{pk} and R_{vk} can be considered as reduced values of the R_{pkx} and R_{vkx} characteristics. The peak zone and the are the initial material portion values of the valley zone in percent. The small value of the former and the large value of the latter represent the ideal load-bearing capacity of the machined surface [20]. These characteristics provide information about the subsequent load-bearing capacity of the machined parts [21].

The history of 3D surface characterization dates to the 1980s, when K.J. Stout and his team at Coventry Polytechnic developed a hardware system and supporting software that became the prototype for the first commercially available software package by providing a wide range of surface visualization techniques. The development of the technology did not go smoothly, as instrument manufacturers believed 3D topography was a 'scientific curiosity' and had no place in industry [22]. After initial wing-boning, the next milestone came in 1990 when, with the support of the European Community, a report of more than 300 pages was published by the University of Birmingham, which proposed the use of 14 3D surface roughness parameters describing the functional, spatial and amplitude properties of the surface. The first touch probe manufacturer was Somicronic, which made a wide range of parameters available on its system. The 'Birmingham 14' parameters were then installed on Somicronic's 3D surface tester in 1996, which included a standard file format that could be transferred to other computer systems [22]. In parallel with European research, advances were also being made in the USA, notably in the development of optical interferometric systems. The main instrument manufacturers were WYKO and ZYGO, whose instruments were capable of extremely fast 3D surface measurements for the capabilities of the time, using techniques such as vertical scanning interferometry or extended range interferometry, while achieving sub-nanometre resolution. At the beginning of the 2000s, instruments using triangulation and confocal techniques began to appear, for example from a company called Scantron [22].

The parameters of the Abbot-Firestone curve are effective for tribological applications [23]. Here, too, the setting of the correct parameters during measurement is crucial [24]. The characteristics of the previously described 2D

Abbott-Firestone curve can also be investigated in the 3D case. For 3D features, Heidari and Yan presented a similar diagram (Figure 6) [25].

These are as follows:

- S_k: core height
- S_{pk}: reduced peak height
- S_{vk}: reduced valley height

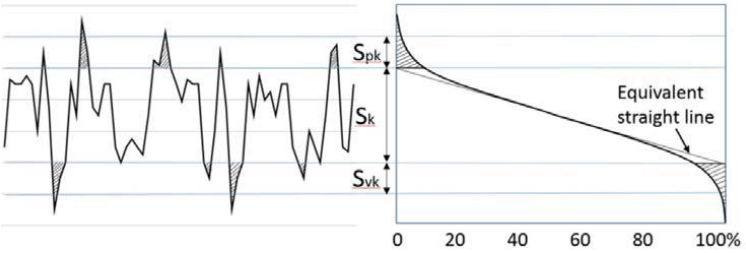

Figure 6. Definition of parameters S_{pk}, S_k and S_{vk} in a bearing area curve [25]

As in the 2D case, the S_{mr1} characteristic defines the boundary between the peak zone and the core zone, while the S_{mr2} portion of material defines the boundary between the core zone and the valley zone.

The surface roughness was measured with an AltiSurf®520 roughness measuring device, located in the Metrology Laboratory of the Institute of Manufacturing Sciences of the University of Miskolc. The measuring machine can move along three perpendicular x-y-z motorised DC axes at 200 mm per axis. Its maximum speed is 40 mm/sec, up to a scale of 0.1 μm [26].

A detailed analysis of the surface topography was performed using the AltiMap software provided with the measuring machine. Among several sensors of the machine, the non-contact interferometric triangular laser was used.

2.5. Calculation of the improvement factors

The improvement factors are used to look for parameters of diamond burnishing where, in addition to the machining being adequate in terms of energy efficiency, the greatest improvement in surface quality after turning was achieved with diamond burnishing.

The required improvement factor is calculated using equation (3), which is a percentage value that gives the improvement in surface quality due to diamond burnishing. This is necessary because the turning process produces surfaces of different quality, which are the starting points for diamond burnishing. The formula is a generalisation formula, with the 'x' replacing the letters 'R' used for 2D surface finishes and 'S' for 3D finishes, and the 'y' generalising the subscripts for the different gauge types.

$$IX_y = \frac{X_{y;turning} - X_{y;burnishing}}{X_{y;burnishing}} \cdot 100\ [\%] \quad (3)$$

2.6. Calculation of K-coefficients

The values of the individual features of the Abbott-Firestone curve do not necessarily give an indication of the quality and properties of the surface, but their relative values, their ratios, their percentage distribution may be of more interest in the context of diamond burnishing. For this purpose, so-called K-coefficients are calculated using the formulas (4)–(9) [27].

$$K_{Rk} = \frac{R_k}{R_k + R_{pk} + R_{vk}} \quad (4)$$

$$K_{Rpk} = \frac{R_{pk}}{R_k + R_{pk} + R_{vk}} \quad (5)$$

$$K_{Rvk} = \frac{R_{vk}}{R_k + R_{pk} + R_{vk}} \quad (6)$$

$$K_{Sk} = \frac{S_k}{S_k + S_{pk} + S_{vk}} \quad (7)$$

$$K_{Spk} = \frac{S_{pk}}{S_k + S_{pk} + S_{vk}} \quad (8)$$

$$K_{Svk} = \frac{S_{vk}}{S_k + S_{pk} + S_{vk}} \quad (9)$$

For example, formula (4) illustrates in percentage form the core roughness depth (R_k) of the roughness profile ($R_k + R_{pk} + R_{vk}$) with respect to the total roughness profile.

3. The analysis of the abbott-firestone curve

3.1. Improvement factors for the surface roughness characteristics of the abbott-firestone curve

The repeatedly mentioned Abbott-Firestone curve characteristics are plotted as a function of feed rate, burnishing speed and burnishing force for comparison with the improvement factors calculated in the previous chapter. To better follow the plots, trend lines were plotted for each data point set, which resulted in mostly similar curves.

In the graphs of the core part of the roughness profile (Figure 7), the magnitude of the improvement factor increases steadily with increasing burnishing force until it reaches a maximum point from which it starts to decrease. This is consistent with our previous observations for the other surface roughness metrics. The plots - especially the plot analysing the 3D parameter - also show that for the

same burnishing rates (red-blue and green-yellow trend lines) the maximum position of the curves, i.e. the burnishing force, is the same, but they differ only in the values of the improvement factor.

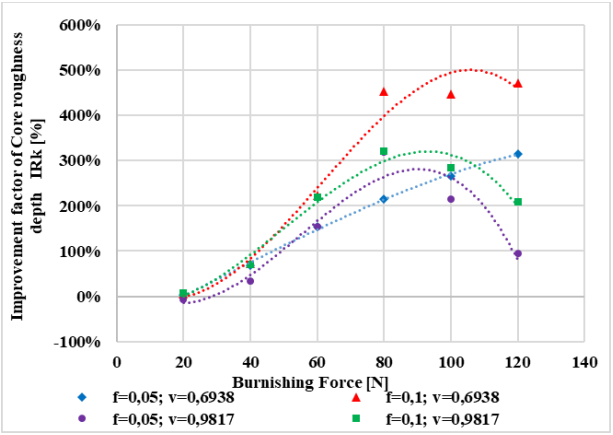

a)

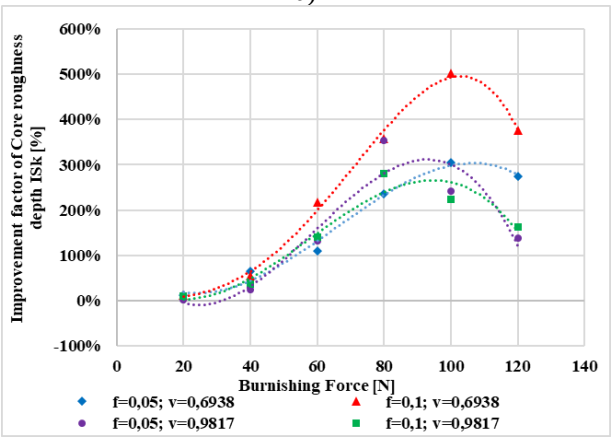

b)

Figure 7. Improvement factor of the core roughness depth as a function of burnishing speed, feed rate and burnishing force, a) 2D case b) 3D case

The improvement factors of the reduced peak height show a much larger variation depending on the variation of the technological parameters (Figure 8). The reduced peak height represents the top of the profile, proportional to the material portion of the core zone and the valley zone. This factor is better evaluated only for the 3D case, as the 2D data did not give a valuable picture of the subject. It can be

observed that at the minimum feed rate and burnishing speed (blue trend line), the improvement factor increased steadily with increasing burnishing force, whereas at the maximum values of these parameters (green trend line), increasing burnishing force even worsened the peak part of the roughness profile over time. On the other hand, for the minimum-maximum combination of values (red, yellow trend lines), the improvement factor was again at its maximum value, with a similar slight improvement above 70-80 N of burnishing force.

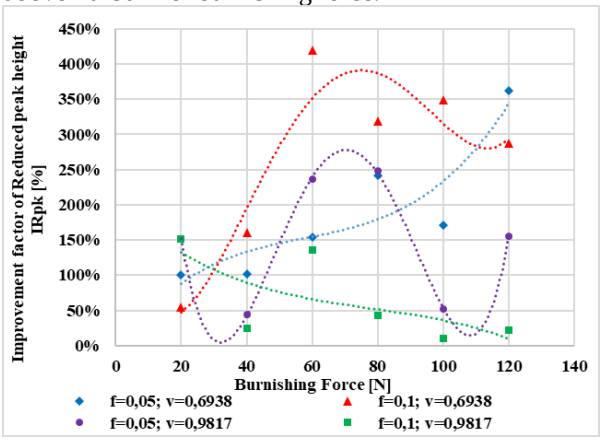

a)

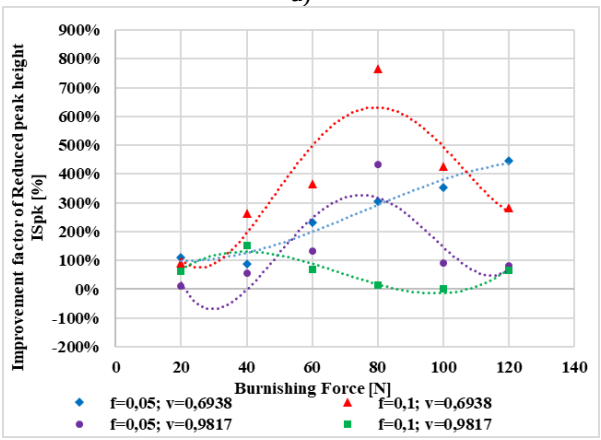

b)

Figure 8. Improvement factor of the reduced peak height as a function of burnishing speed, feed rate and burnishing force, a) 2D case b) 3D case

As with the peak section, the improvement factors in the valley portion of the Abbot-Firestone curve varied quite a bit with changes in process parameters (Figure 9). The valley portion of the barrel surface provides feedback from the deepest layers of the surface. As in the peak part of the profile, again relying only on the 3D metric, it can be observed that increasing the burnishing force first has a negative effect on the improvement factor (negative values also occur), while reaching a minimum point, the highest burnishing forces already improve the valley part of the barrel surface curve to a large extent. From this, therefore, we can draw the important conclusion that the deepest "valleys" on the surface are in fact only reduced by diamond burnishing when sufficiently high forces are applied.

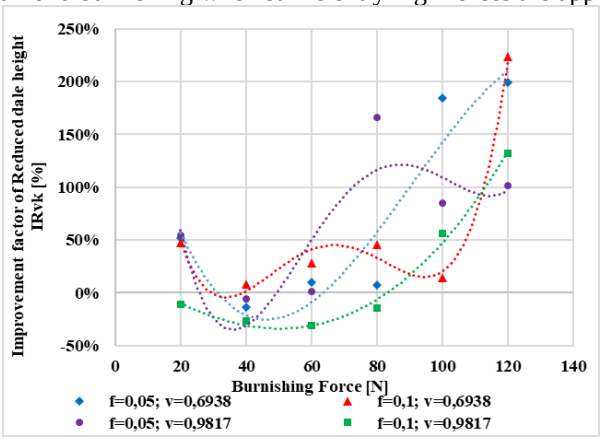

a)

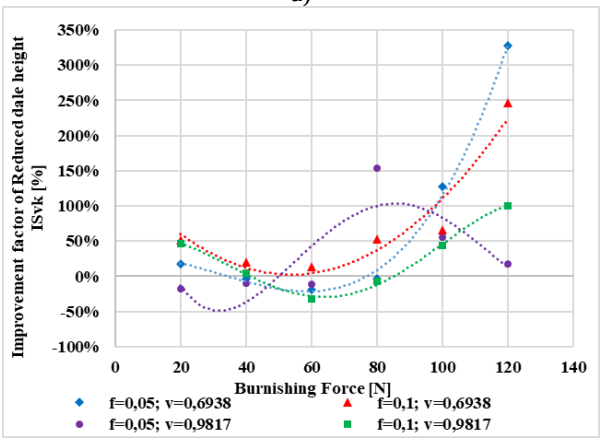

b)

Figure 9. Improvement factor of the reduced valley height as a function of burnishing speed, feed rate and burnishing force, a) 2D case b) 3D case

3.2. K-coefficients of the surface roughness characteristics of the abbott-firestone curve

The K-coefficients calculated in the previous chapter are plotted as a function of the burnishing force in the following figures. First, let us consider the core roughness depth to the roughness profile, as shown in the 2D and 3D cases in Figure 10. In both dimensions, similar conclusions can be drawn from the plotted trend lines, as diamond burnishing after turning has reduced the proportion of this part in the surface profile by 10-20% except for the smallest burnishing force. It is also seen that the ratio has a minimum at 60 and 80 [N], from where the ratio starts to increase with further increase of the burnishing force. This suggests that too high and burnishing force no longer improves the surface quality.

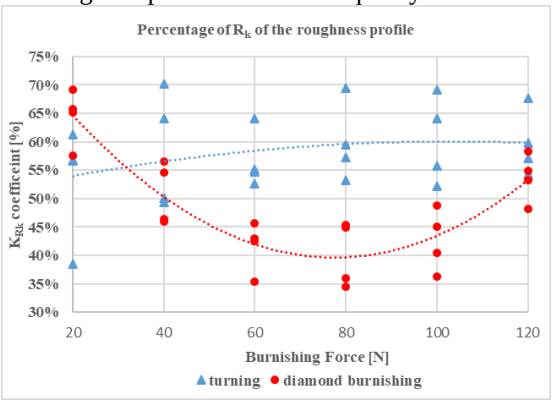

a)

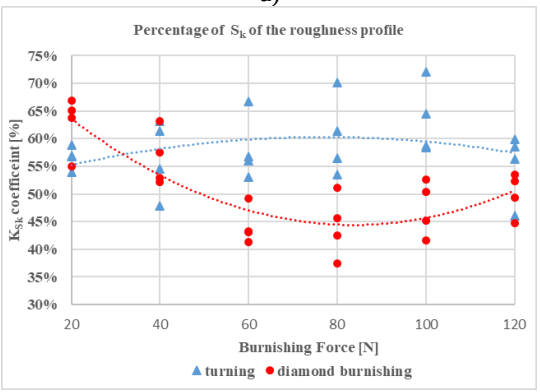

b)

Figure 10. Percentage of the core roughness depth of the roughness profile in the Abbott-Firestone curve as a function of the burnishing force, a) 2D case b) 3D case

And if we recall formula (2), where the power requirement for diamond burnishing was calculated as the product of the burnishing power and the burnishing speed, we can see that in this case, lower burnishing power not only requires better surface quality, but also lower power, which is a clear objective in terms of sustainability and energy efficiency. Following the core part, the reduced peak height of the roughness profile was investigated, as shown in Figure 11, also for 2D and 3D cases. We found, as shown in the figures, that the peak portion of the barrel surface curve was also reduced by 8-10% by diamond burnishing, interestingly just except for the highest burnishing force. Again, this is positive feedback, as our goal in diamond burnishing is to reduce this portion, to "fill in" the valley portion of the roughness profile, thus making the surface more compact. As the lower burnishing force was also more favourable for the surface quality, the energy efficiency principles are also satisfied, as lower power requirements resulted in better surface quality parameters.

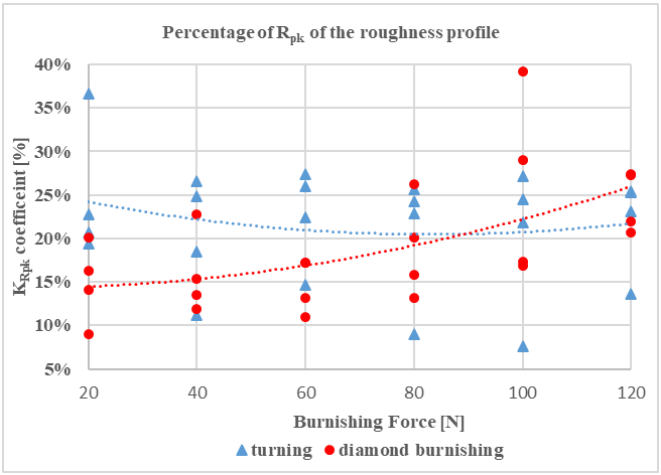

a)

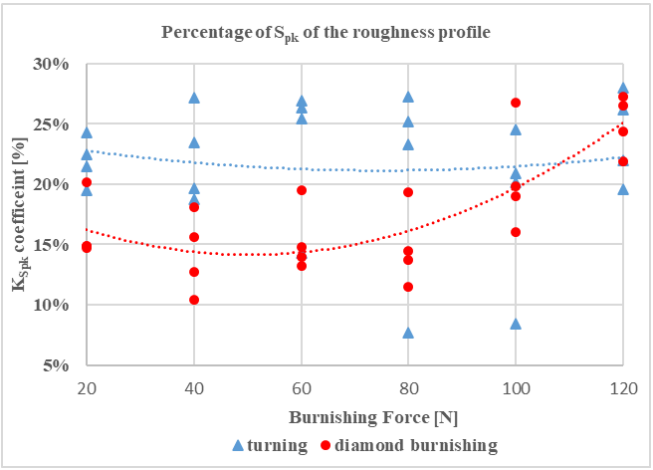

b)

Figure 11. Percentage of the reduced peak height of the roughness profile in the Abbott-Firestone curve as a function of the burnishing force, a) 2D case b) 3D case

Finally, look at Figure 12, where the ratio of the valley portion of the roughness profile is examined in 2D and 3D. In contrast to the previous two cases, our aim is to increase the proportion of the valley section in diamond burnishing, and as can be seen in the figure, this is achieved in almost all cases, in some cases improving the proportion by 20%. It can also be seen that, again, the best results are obtained for the 60-80 [N] burnishing forces, i.e. those where the valley section will have the highest proportion of the roughness profile. Considering this in the context of energy efficiency, we can also conclude that it satisfies its principles.

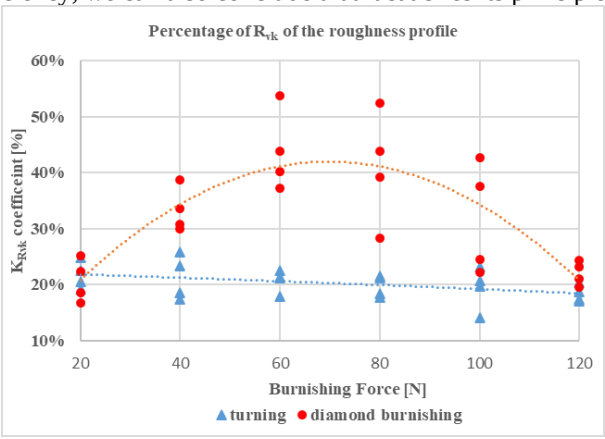

a)

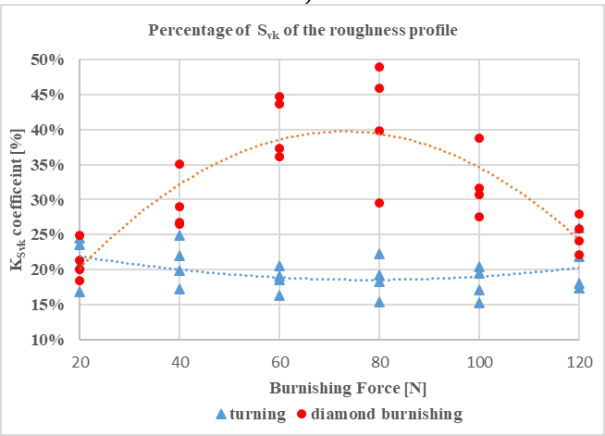

b)

Figure 12. Percentage of the reduced valley height of the roughness profile in the Abbott-Firestone curve as a function of the burnishing force, a) 2D case b) 3D case

4. Summary

In the research we provided an overview of the context of the topic, starting from the issues of energy efficiency, environmental awareness, and sustainable development. We examined the positive properties of alternative machining methods, such as diamond burnishing, and looked at the substrate surface, which is key to the relationship between surface quality and diamond burnishing. In the first part of the paper, we introduced the science of sustainable development, industrial ecology, and its various systems models, and then turned to the three pillars of sustainable development. The relationship between energy and eco-efficiency, their characteristics and recent research results were discussed. In the next section, we described the dimensions and material quality of the test specimens that were tested. The technological characteristics of the turning and diamond-burnishing processes were then presented. The characteristics and usefulness of the barrel Abbott-Firestone curves were discussed in detail and the improvement factors and K-coefficients were calculated. In the third part, we have presented in detail the experimental results obtained by examining the data of the Abbott-Firestone curves. Using the improvement factors, we could see from the diagrams of the core part of the roughness profile that as the burnishing force is increased, the improvement factor increases steadily until it reaches a maximum point from which it starts to decrease. By examining the valley part of the profile, we have seen that the deepest "valleys" in the surface are only reduced by diamond burnishing when a sufficiently

high force is applied. However, by also looking at the K-coefficient data, we found that lower burnishing forces often favour surface quality over higher burnishing forces, which also reduces the power requirements of machining, creating optimal energy efficiency during diamond burnishing. Our aim was to reduce the peak or core fraction and increase the valley fraction in diamond burnishing, and as we have seen in the figures, we have achieved this in almost all cases, in some cases improving the ratios by 20%. In all cases, the best results were obtained with burnishing forces of 60-80 [N], with both lower and higher burnishing forces worsening the ratios. These results therefore fully satisfy the main energy efficiency guidelines.

References: **1**. *P. Bartelmus, S. Moll, S. Bringezu, S. Nowak, R. Bleischwitz*: Translating sustainable development into practice: a 'patchwork' of some new concepts and an introduction to material flows analysis in: Emiel F.M. Wubben (ed.) Green and Competitive: Ending the Stalemate, Chapt. 1, pp. 1–38, Edward Elgar Publishing. 2004. **2.** *D.H. Meadows, J. Randers, D.L. Meadows:* The limits to growth. Chelsea Green Publishing, USA. 2004. **3.** Brundtland Commission: Our Common Future. Oxford University Press, Oxford, UK. 1987. **4.** *S. Schaltegger, A. Sturm:* Ökologieinduzierte Entscheidungsprobleme des Managements: Ansatzpunkte zur Ausgestaltung von Instrumenten. WWZ-Discussion Paper No. 8914. 1989. **5.** UN (United Nations): Earth Summit. Agenda 21. The United Nations Programme of Action from Rio., (Ed.) United Nations Department of Public Information New York. 1992. **6.** *B.R. Allenby*: Industrial Ecology – Policy Framework and Implementation, Englewood Cliffs, NJ: Prentice Hall. 1999. **7.** *C. Herrmann:* Ganzheitliches Life Cycle Management - Nachhaltigkeit und Lebenszyklusorientierung in Unternehmen. Springer Verlag, Berlin, Germany. 2010. **8.** *M.E. Porter, C.v.d. Linde:* 'Green and Competitive: Ending the Stalemate', in E.v.d. Wubben (ed.), The Dynamics of the Eco-Efficient Economy, Cheltenham, UK and Northampton, MA: Edward Elgar, pp. 33–55. 2001. **9.** *R. Bleischwitz:* 'Governance of Eco-Efficiency in Japan – An Institutional Approach', International Asian Quarterly, 34 (1–2), 107–26. 2003. **10.** *R. Bleischwitz, P. Hennicke:* Eco-efficiency, regulation and sustainable business: Towards a governance structure for sustainable development. pp. 1–228. ESRI Studies Series on the Environment, Germany 10.4337/9781845420574.00001. 2004. **11.** *L.D. DeSimone, F. Popoff:* Eco-Efficiency: The Business Link to Sustainable Development, vol. 1, 1 ed., The MIT Press. 2000. **12.** DIN EN ISO 14040: Umweltmanagement - Ökobilanz - Grundsätze und Rahmenbedingungen (ISO 14040:2006). Beuth Verlag, Berlin, Germany. 2009. **13.** DIN EN ISO 14045, Umweltmanagement - Ökoeffizienzbewertung von Produktsystemen - Prinzipien, Anforderungen und Leitlinien (ISO 14045:2012). Beuth Verlag, Berlin, Germany. 2012. **14.** *R. Heijungs:* From thermodynamic efficiency to eco-efficiency. In: Huppes, G., Ishikawa, M. (eds) Quantified Eco-Efficiency. Eco-Efficiency in Industry and Science, vol 22. Springer, Dordrecht. 2007. **15.** https://www.inoxservice.hu/upload/inline/adatlapok/durvalemezek/ 1.4307%20-%20ADATLAP.pdf (2024. 04. 15) **16.** *L. Gribovszki*, Mechanical processing (Tankönyvkiadó, Budapest, pp. 418-421. 1977. (In Hungarian) **17.** *G. Varga, S. Smolnicki, M. Babič, W. Caesarendra*, Energy Efficiency Analysis When Grinding and Diamond Burnishing of Components, In: Gençyılmaz, M. Güneş; Durakbasa, Numan M. (ed.-s.) Towards Industry 5.0: Selected Papers from ISPR2022, Cham, Switzerland, Springer International Publishing pp. 378-396. 2023. **18.** *V. Ferencsik*, Analytical analysis of the theoretical surface roughness in the case of burnishing of cylindrical workpiece, Rezanie i Instrument v Tehnologiceskikh Sistemakh / Cutting and Tool in Technological Systems 99 pp. 101–109, (2023). **19.** https://perfor.hu/erdesseg_67 (2024. 04. 15.) **20.** *I. Szalóki, S. Sipos, Z.J. Viharos:* Analysis of the milled surface structure of syntactic metal foams. In: Proceedings of 8th International Engineering Symposium at Bánki (IESB 2016). Óbudai Egyetem, Budapest, pp. 1–21. ISBN 978-615-5460-95-1. 2016. (In Hungarian) **21.** *D. Kubatova, M. Melichar*: Roughness Evaluation Using Abbott-Firestone Curve

Parameters, Proceedings of the 30th DAAAM International Symposium, pp. 0467–0475, B. Katalinic (Ed.), Published by DAAAM International, ISBN 978-3- 902734-22-8, ISSN 1726-9679, Vienna, Austria. 2019. **22.** *L. Blunt, X. Jiang*: Advanced Techniques for Assessment Surface Topography: Development of a Basis for 3D Surface Texture Standards "Surfstand", Kogan Page Science, pp. 1–355. 2003. **23.** *I. Sztankovics*: Preliminary Study on the Function-Defining 3D Surface Roughness Parameters in Tangential Turning. International Journal of Integrated Engineering 15: 7 pp. 72–81. 2023. **24.** *A. Nagy*: Investigation of the effect of areal roughness measurement length on face milled surface topographies. Cutting and Tools in Technological System, (94), pp.: 60–69. 2021. https://doi.org/10.20998/2078-7405.2021.94.07, **25.** *M. Heidari, J. Yan:* Fundamental characteristics of material removal and surface formation in diamond turning of porous carbon. International Journal of Additive and Subtractive Materials Manufacturing, 1 (1), pp.: 23–41. 2017. **26.** https://www.altimet.fr/?page_id=236&lang=en (2024. 04. 15.) **27.** *M. Tomov, P. Karolczak, H. Skowronek, P. Cichosz, M. Kuzinovski:* Mathematical Modelling of Core Roughness Depth During Hard Turning. In: Królczyk, G., Niesłony, P., Królczyk, J. (eds) Industrial Measurements in Machining. IMM 2019. Lecture Notes in Mechanical Engineering. Springer, Cham. 2020. https://doi.org/10.1007/978-3-030-49910-5_1

Сілард Смольницькі, Дьюла Варга, Мішкольц, Угорщина

АНАЛІЗ КРИВОЇ ЕББОТА-ФАЙЄРСТОУНА НА ПОЛІРОВАНІЙ АЛМАЗНИМ ВИГЛАДЖЕННЯМ ПОВЕРХНІ

Анотація. *У дослідженні ми надали огляд контексту теми, починаючи з питань енергоефективності, екологічної свідомості та сталого розвитку. Ми розглянули позитивні властивості альтернативних методів обробки, таких як алмазне полірування, і звернули увагу на поверхню підкладки, яка є ключовим фактором у взаємозв'язку між якістю поверхні та алмазним поліруванням. У першій частині статті ми представили науку сталого розвитку, промислову екологію та її різні системні моделі, а потім звернулися до трьох стовпів сталого розвитку. Було обговорено взаємозв'язок між енергетичною та екологічною ефективністю, їхні характеристики та останні результати досліджень. У наступному розділі ми описали розміри та якість матеріалу дослідних зразків, які були випробувані. Потім були представлені технологічні характеристики процесів точіння та алмазного вигладжування. Детально обговорено характеристики та корисність кривих Еббота-Файрстоуна, а також розраховано коефіцієнти покращення та К-коефіцієнти. У третій частині ми детально представили експериментальні результати, отримані при вивченні даних кривих Еббота-Файрстоуна. Використовуючи коефіцієнти поліпшення, ми могли бачити з графіків основної частини профілю шорсткості, що зі збільшенням сили полірування коефіцієнт поліпшення неухильно зростає, поки не досягне максимальної точки, з якої він починає зменшуватися. Вивчаючи долинні частини профілю, ми побачили, що найглибші "долини" на поверхні зменшуються за допомогою алмазного полірування вигладженням лише за умови застосування досить високої сили. Однак, проаналізувавши дані про коефіцієнт К, ми виявили, що менші зусилля полірування часто сприяють поліпшенню якості поверхні, ніж більші зусилля, що також знижує енергоспоживання при обробці, створюючи оптимальну енергоефективність під час алмазного полірування. Наша мета полягала в тому, щоб зменшити частку піків або серцевини і збільшити частку долини при алмазному вигладжувальному поліруванні, і, як ми бачимо на рисунках, ми досягли цього майже у всіх випадках, в деяких випадках покращивши співвідношення на 20%. У всіх випадках найкращі результати були отримані при силі притискання 60-80 [Н], причому як менші, так і більші сили притискання погіршували співвідношення. Таким чином, ці результати повністю задовольняють основним рекомендаціям з енергоефективності.*

Ключові слова: *енергоефективність; сталий розвиток; вигладжувальне алмазне полірування; обробка поверхні.*